Available online at www.ilcpa.pl

International Letters of Chemistry, Physics and Astronomy

2 (2012) 7-14 ISSN 2299-3843

The pecularities of structure and diffraction by misfit mixed-layer nanotubes

Oleg Figovsky[1], Dmitry Pashin[2], Zufar Khalitov[2], Diana Valeeva[2] and Andrey Chkanov[2]

[1]International Nanotechnology Research Center "Polymate", Migdal Haemek 23100, Israel
[2]Kazan National Research Technical University, 10, K. Marx str., Kazan, Tatarstan 420111, Russia

E-mail address: pashin@addnano.ru

ABSTRACT

The analysis of diffraction by separate mixed-layer goffered nanotube's lattice is offered. Two extreme cases of the large and small size of coherent scattering regions (CSR) in a radial direction are considered. The qualitative explanation of observed diffraction effects is given.

Keywords

nanotube, goffered nanotube, superlattice.

1. INTRODUCTION

The misfit mixed-layer nanotubes SnS_2/SnS with a various degree of ordering in cylindrical layers SnS_2 and SnS alternation were synthesized in the Weizmann Institute of Science (Israel) by R. Tenne group [1]. Nanotubes were synthesized on the basis of flat layered crystals SnS_2 by extraction of a part of S atoms and forming SnS layers. The misfit of layers SnS_2 and SnS, having not only various parameters of lattices, but also symmetry of layer, results in a curvature of flat packs and forming nanotubes.

During an experimental research the nanotubes with rather original structure were found, on the TEM-images of which the periodically alternating in a longitudinal direction of nanotube light and dark radial (or nearly so radial) strips were observed (fig. 1 and 2, violet line – nanotube axis, light-blue - zero layer line). More detailed analysis of the TEM-images has shown, that within the strips the layers have wavy character, and the radius of layers curvature is approximately constant. Hence, to coordinate the lattices the nanotubes layers are bent not only in a direction of the cylinder's circle, but also in direction of its axis, forming, thus, goffered nanotube. Originally such nanotubes were named "strained", however term "goffered" more corresponds to character of structure.

It is obvious, that such way of coordination is possible only for the layers with close longitudinal (along a nanotube's axis) parameters of lattices a [2]. The analysis of microdiffraction patterns has shown, that two types of layers SnS_2 always take place in SnS_2/SnS nanotubes: with a = 0,36 nm and developed on $\pi/2$ with a = 0,63 nm, while the parameter a of SnS layer is equal 0,58 nm. Apparently, the additional bend in a direction of nanotube's axis

arises in pair of layers SnS_2 and SnS, where the layer SnS_2 has a = 0,63 nm, and this layer is positioned on the external side of the bend. Really, the goffering takes place only in mixed-layer nanotubes OT (O - SnS layer, T - SnS_2 layer) and is absent in structures OTT or OTOTT, where the presence of an additional SnS_2 layer interferes with a bend.

The "additional" layer lines with reflexes are distinctly observed in the microdiffraction patterns of goffered nanotubes (fig. 1 and 2). Similar additional layer lines, located close to basic ones, are known in superlattices diffraction researches. It allows to offer the model of nanotube structure, based on a wavy superlattice in a longitudinal direction, and to apply the known approaches to interpretation its diffraction pattern. The measurements have shown, that, as in usual superlattices, inverse value of distance Δ_s from the basic layer line up to additional one (fig. 1) well corresponds to longitudinal periodicity in the TEM-image, equal ≈ 5,4 nm.

The microdiffraction patterns on fig. 1 and 2 are rather similar, however there is an essential difference. The distribution of intensity on an additional layer line near to basic layer line 20l on fig. 1 is similar to a profile of the basic line. The analogous distributions on microdiffraction pattern of goffered nanotube on fig. 2 have obvious displacements in a direction of nanotube's axis. Interpretation of this effect requires theoretical research of a problem.

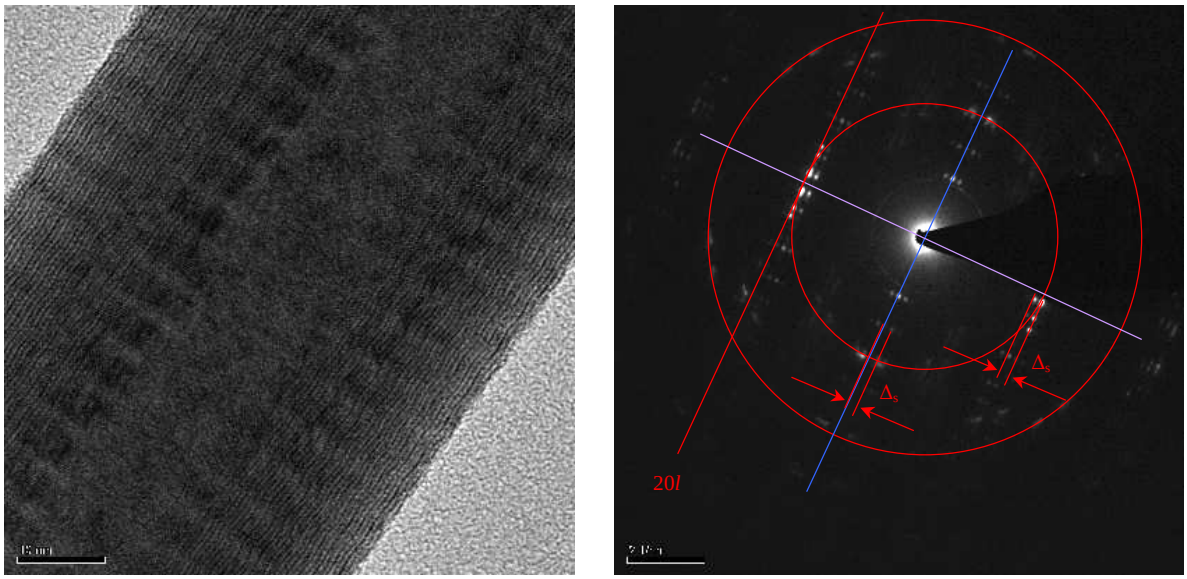

Fig. 1. TEM-image, microdiffraction pattern and sublattices scheme of SnS_2-SnS nanotube with thick radial CSR.

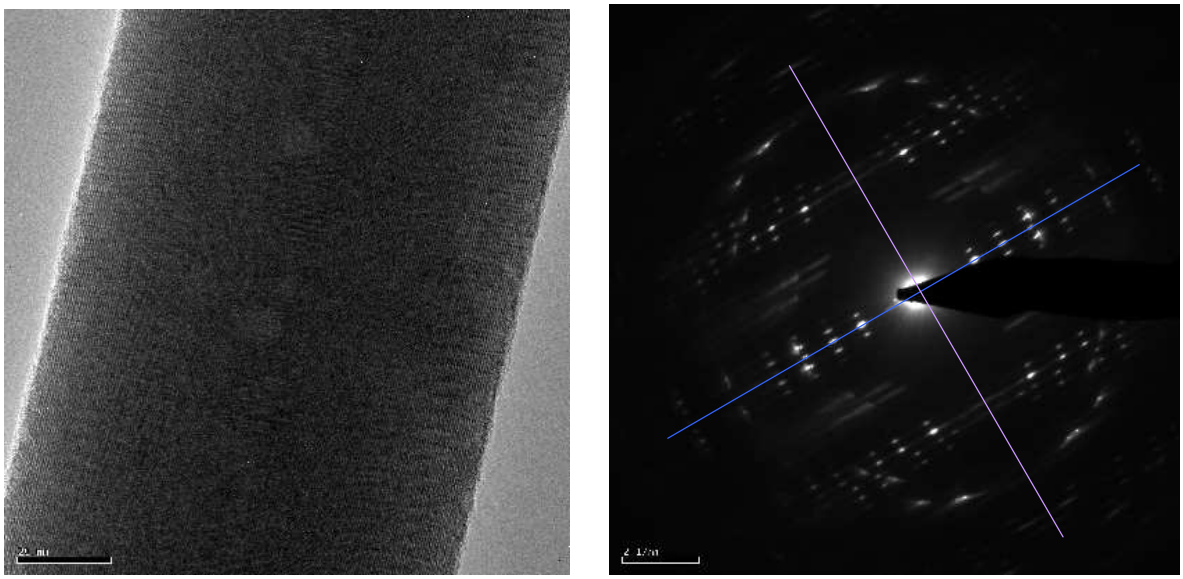

Fig. 2. TEM-image and microdiffraction pattern of SnS_2-SnS nanotube with thin radial CSR.

As a first step let's consider positions of the lattice sites of circular orthogonal [2] goffered nanotube, shown on a fig. 3 with the basic designations, and basic features of diffraction by it.

2. THE LATTICE OF GOFFERED NANOTUBE

Let nanotube, oriented along axis *z*, consists of the ordered alternating "goffered" pairs of layers type of *A* and *B*, having the superperiod λ and radius of the goffer bend r_g. Let both layers of every *m*-th pair has the same centre of goffer curvature, located on a circle of radius O_m (fig. 3). Let the radius of internal layer's point, most remote from nanotube's axis, is equal ρ_0, d_A and d_B - thickness of layers *A* and *B*, accordingly, and $d = d_A + d_B$.

The discussed way of the coordination means that $\Delta\varepsilon$ - an angle, under which the coordinated cell of pair layers is visible from the centre of curvature of pair, becomes the crystallographic constant. Longitudinal parameter *a* of a lattice of coordinated layers pair has no definite value and for convenience can be chosen on an internal surface of pair.

Let's number the sites of lattice, formed by pairs, within the limits of superlattice's wave by integer variable *t*, and waves - by *n*. Then the angular position ε_t of any pair's sites concerning their centre of curvature is possible to write down as:

$$\varepsilon_t = \Delta\varepsilon t - \varepsilon, \qquad t = 0 \div T - 1,$$

where $\Delta\varepsilon = \dfrac{a}{r_g}, \qquad \varepsilon = \arcsin\dfrac{\lambda}{2\left(r_g + d\right)},$

and *z*-coordinates of these sites and number of cells on the length of wave – as:

$$z_{nt} = n\lambda + \frac{\lambda}{2} + r_g \sin\varepsilon_t, \quad T = \frac{2r_g\varepsilon}{a}, \qquad (1)$$

under obvious condition $\lambda \le 2r_g$.

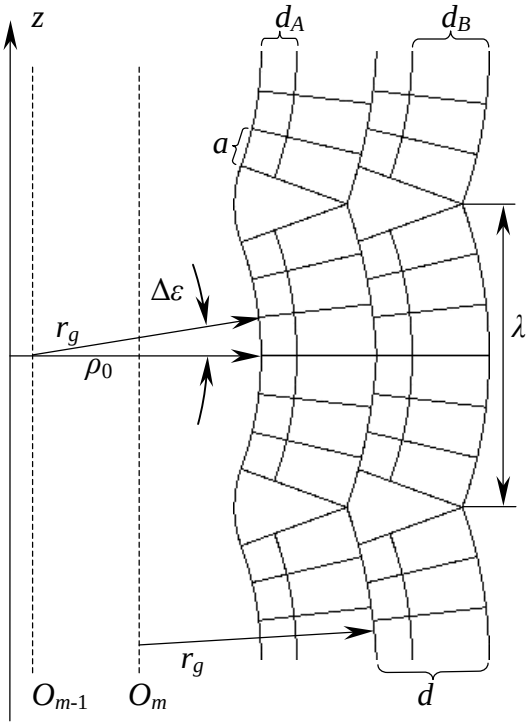

Fig. 3. The basic designations in goffered nanotube.

Radius of circles, on which the centres of curvature of an internal layer's waves are located, is equal to $\rho_0 - r_g$. Hence, it is possible to write down the polar radiuses of sites of considered lattice as:

$$\rho_{mt} = \rho_m - r_g + r_g \cos\varepsilon_t, \qquad \rho_m = \rho_0 + md. \qquad (3)$$

From here we can find an angle, under which the circular parameter *b* at $\varepsilon_t = 0$ is seen from the nanotube's axis, and by it - the angular positions of sites:

$$\varphi_{mv} = \frac{b}{\rho_m}v + \varepsilon_m, \qquad v = 0 \div p_m - 1, \qquad p_m = \frac{2\pi\rho_m}{b}, \qquad (4)$$

where *v* - number of site on the circle, p_m - number of sites on the *m*-th pair's circles (integer by definition), ε_m - initial azimuthal angular phase of the appropriate layer. It is obvious, that the circular parameter *b* has some variation within the limits of superlattice wavelength λ in considered model. However it is known [3], that this parameter does not influence on circular nanotube's strong ($k = 0$) reflexes, which consideration is the purpose of research.

3. THE STRONG REFLEXES AMPLITUDE

Let's write down an amplitude of diffraction by lattice, defining by expressions (1), (3) and (4), in cylindrical coordinates system $\{R, \varphi^*, z^*\}$ in reciprocal space:

$$A(R,\varphi^*,z^*)=\sum_{m,n,v,t}\exp\{2\pi i[R\rho_{mt}\cos(\varphi_{mv}-\varphi^*)+z_{nt}z^*]\}=$$

$$=\sum_{n=0}^{N-1}\exp(2\pi i\lambda z^* n)\sum_{t=0}^{T-1}\exp\left[2\pi i\left(\frac{\lambda}{2}+\beta_t\right)z^*\right]\sum_{m=0}^{M-1}\sum_{v=0}^{p_m-1}\exp[2\pi iR\rho_{mt}\cos(\varphi_{mv}-\varphi^*)], \quad (5)$$

where $\beta_t = r_g \sin\varepsilon_t$, (6)

M and N - number of layer pairs in nanotube and its length (in units λ), accordingly. Sum over goffer periods (over n) is easily calculated and has sharp maxima, equal to N, at

$$\pi\lambda z^* = h_1\pi \quad \Rightarrow \quad z^*=\frac{h_1}{\lambda}, \qquad h_1 = 0,\pm1,\pm2,\ldots. \quad (7)$$

The expression (7) defines the system of layer planes in reciprocal space, on which all sites of reciprocal lattice take place. In a plane $\{R, z^*\}$, that is in the section of these planes by Evald sphere, that corresponds to the usual electron microdiffraction experiment, it gives the system of close located to each other layer lines (7), which numbering is the same with values of index h_1. Let's be limit by half plane $z^* \geq 0$, that means $h_1 \geq 0$.

With taking into account (7) amplitude transforms in:

$$A(R,\varphi^*,h_1)=N(-1)^{h_1}\sum_{t=0}^{T-1}\exp\left(2\pi i\frac{h_1}{\lambda}\beta_t\right)\sum_{m=0}^{M-1}\sum_{v=0}^{p_m-1}\exp[2\pi iR\rho_{mt}\cos(\varphi_{mv}-\varphi^*)]. \quad (8)$$

Let's expand the second exponent in (8) into a series of cylindrical waves according to

$$\exp(i\alpha\cos\gamma)=J_0(\alpha)+2\sum_{q=1}^{\infty}i^q\cos(q\gamma)J_q(\alpha). \quad (9)$$

$$A(R,\varphi^*,h_1)=N(-1)^{h_1}\sum_{t=0}^{T-1}\exp\left(2\pi i\frac{h_1}{\lambda}\beta_t\right)\sum_{m=0}^{M-1}J_0(2\pi R\rho_{mt})\sum_{v=0}^{p_m-1}1+$$

$$+2N(-1)^{h_1}\sum_{t=0}^{T-1}\exp\left(2\pi i\frac{h_1}{\lambda}\beta_t\right)\sum_{m=0}^{M-1}\sum_{v=0}^{p_m-1}\sum_{q=1}^{\infty}i^q\cos[q(\varphi_{mv}-\varphi^*)]J_q(2\pi R\rho_{mt})=A_S+A_D,$$

where, in view of triviality of sum over v, the first addendum looks like

$$A_S(R,h_1)=N(-1)^{h_1}\sum_{t=0}^{T-1}\exp\left(2\pi i\frac{h_1}{\lambda}\beta_t\right)\sum_{m=0}^{M-1}p_m J_0(2\pi R\rho_{mt}) \quad (10)$$

and gives the amplitude of so-called "strong " reflexes [3].

With the purpose of estimation of strong reflexes intensity distribution let's approximate the Bessel function in (10) by cosine:

$$J_0(x)\approx\sqrt{\frac{2}{\pi x}}\cos x$$

and, neglecting by dependence on t under a radical, let's change the sums by places:

$$A_S(R,h_1)\approx N(-1)^{h_1}\sum_{m=0}^{M-1}\frac{p_m}{\pi\sqrt{R\rho_m}}\sum_{t=0}^{T-1}\exp\left(2\pi i\frac{h_1}{\lambda}\beta_t\right)\cos(2\pi R\rho_{mt}).$$

Let's consider the sum over t, having presented cosine in an exponential form:

$$\frac{1}{2}\sum_{t=0}^{T-1}\exp\left(2\pi i\frac{h_1}{\lambda}\beta_t\right)\left[\exp(2\pi iR\rho_{mt})+\exp(-2\pi iR\rho_{mt})\right]=\frac{1}{2}(S_1+S_2),$$

where $S_1=\sum_{t=0}^{T-1}\exp\left[2\pi i\left(\frac{h_1}{\lambda}\beta_t+R\rho_{mt}\right)\right]$, $S_2=\sum_{t=0}^{T-1}\exp\left[2\pi i\left(\frac{h_1}{\lambda}\beta_t-R\rho_{mt}\right)\right]$. (11)

With taking into account (3) and (6), the sum S_1:

$$S_1=\exp\left[2\pi iR(\rho_0-r_g+md)\right]\times$$

$$\times\sum_{t=0}^{T-1}\exp\left[2\pi ir_g\frac{h_1}{\lambda}\sin(\Delta\varepsilon t-\varepsilon)\right]\exp\left[2\pi ir_gR\cos(\Delta\varepsilon t-\varepsilon)\right]. \quad (12)$$

Let's expand two last exponents into a series of cylindrical waves according to

$$\exp(i\alpha\sin\gamma)=J_0(\alpha)+2\sum_{q=1}^{\infty}\cos(2q\gamma)J_{2q}(\alpha)+2i\sum_{q=0}^{\infty}\sin[(2q+1)\gamma]J_{2q+1}(\alpha)$$

and $\exp(i\alpha\cos\gamma)=\sum_{q=-\infty}^{\infty}i^qJ_q(\alpha)\exp(iq\gamma)$.

Then $S_1=\exp\left[2\pi iR(\rho_0-r_g+md)\right](S_0+S_c+S_s)$,

where $S_0=J_0\left(2\pi r_g\frac{h_1}{\lambda}\right)\sum_{q'=-\infty}^{\infty}i^{q'}J_{q'}(2\pi r_gR)\exp(-iq'\varepsilon)\sum_{t=0}^{T-1}\exp(iq'\Delta\varepsilon t)=$

$$=J_0\left(2\pi r_g\frac{h_1}{\lambda}\right)\sum_{q'=-\infty}^{\infty}i^{q'}J_{q'}(2\pi r_gR)\exp(-iq'\varepsilon)G_0(q'\Delta\varepsilon), \quad (13)$$

$$S_c=\sum_{q=1}^{\infty}J_{2q}\left(2\pi r_g\frac{h_1}{\lambda}\right)\sum_{q'=-\infty}^{\infty}i^{q'}J_{q'}(2\pi r_gR)\times$$

$$\times\{\exp[-i(q'+2q)\varepsilon]G_c[(q'+2q)\Delta\varepsilon]+\exp[-i(q'-2q)\varepsilon]G_c[(q'-2q)\Delta\varepsilon]\}, \quad (14)$$

$$S_s=\sum_{q=0}^{\infty}J_{2q+1}\left(2\pi r_g\frac{h_1}{\lambda}\right)\sum_{q'=-\infty}^{\infty}i^{q'}J_{q'}(2\pi r_gR)\times$$

$$\times\{\exp[-i(q'+2q+1)\varepsilon]G_s[(q'+2q+1)\Delta\varepsilon]-\exp[-i(q'-2q-1)\varepsilon]G_s[(q'-2q-1)\Delta\varepsilon]\}. \quad (15)$$

Here, as well as earlier, is used the sum of a kind

$$G(x)=\sum_{m=0}^{M-1}\exp(ixm)=\frac{\sin\frac{Mx}{2}}{\sin\frac{x}{2}}\exp\left[i(M-1)\frac{x}{2}\right], \quad (16)$$

which has a sharp maximum at x, equal to an integer of 2π, the height of a maximum is equal to M, and its width is inverse proportional to this value. For example, in the case of S_0: $x = q'\Delta\varepsilon$, $M = T$, the maximum of function is realized at

$$q'=h_2\frac{2\pi}{\Delta\varepsilon}, \qquad h_2=0;\pm1;\pm2;\pm3;... \quad (17)$$

However addendum S_1 of amplitude contains also the multiplier, depending on the index of summation over nanotube's layers (over m). This summation, after rejection of factors, insignificant for this analysis, gives the amplitude's multiplier $G(2\pi Rd)$, which also are looking like (16). Hence, the amplitude of strong reflexes represents a number of addendums, each of

which contains product of functions of a kind (16): $G(2\pi Rd)$ on the one hand, and one of functions $G_0(q'\Delta\varepsilon)$, $G_c[(q' \pm 2q)\Delta\varepsilon]$ and $G_s[(q' \pm 2q \pm 1)\Delta\varepsilon]$ - on another. Last three functions do

not depend on spatial variable R, but influence a choice of the members of series over q', the Bessel functions of which contain this variable.

Thus, the character of an arrangement of amplitude maxima in a scale R depends on the correlation between the widths of functions of a kind (16), which are determined by parameters T and M, in each product: the narrower function determines form and position of diffraction pattern maxima and the wider - modulates their intensities. Let's consider extreme cases of thick and thin radial CSR.

3.1. The thick radial CSR ($M >> T$)

In this case maxima of function $G(2\pi Rd)$ are narrow and intensive and positioned in points of it's extremum:

$$2\pi Rd = 2\pi l \quad \Rightarrow \quad R_l = \frac{l}{d}, \qquad l = 0,\pm1,\pm2,.... \tag{18}$$

It means, that the arrangement of strong reflexes is identical on all layer lines of such nanotube. Such microdiffraction pattern is given in a fig. 1 with the only difference, that it belongs not circular nanotube, which lattice is considered for analysis simplification, but longitudinal monoclinic [2, 3]. Let's compare the relative intensities of layer lines, determined by addendums S_0, S_c and S_s.

Let's consider addendum S_0. Maxima of function $G_0(q'\Delta\varepsilon)$ are in points (17). On the other hand, the main maximum of Bessel function $J_{q'}(2\pi r_g R)$ is close to value of argument, equal to its index, that means, that in points (18) the main maxima of Bessel functions with $q' = 2\pi r_g l/d$ are positioned. It is obvious, that generally this condition can not be satisfied simultaneously with condition (17). It means, that addendum S_0 practically does not influence relative intensity of layer lines.

Addendum S_c in points (18) looks like: $S_c^l = S_{cl}^+ + S_{cl}^-$, where

$$S_{cl}^+ = \sum_{q=1}^{\infty} J_{2q}\left(2\pi r_g \frac{h_1}{\lambda}\right) \sum_{q'=-\infty}^{\infty} i^{q'} J_{q'}\left(2\pi r_g \frac{l}{d}\right) \exp\left[-i(q'+2q)\varepsilon\right] G_c\left[(q'+2q)\Delta\varepsilon\right],$$

$$S_{cl}^- = \sum_{q=1}^{\infty} J_{2q}\left(2\pi r_g \frac{h_1}{\lambda}\right) \sum_{q'=-\infty}^{\infty} i^{q'} J_{q'}\left(2\pi r_g \frac{l}{d}\right) \exp\left[-i(q'-2q)\varepsilon\right] G_c\left[(q'-2q)\Delta\varepsilon\right].$$

The main maxima of Bessel functions of addendum S_{cl}^+ are located close to points $q' \approx 2\pi r_g l/d$ and $2q \approx 2\pi r_g h_1/\lambda$. On the other hand indexes q' and q are connected with each other by area of noticeable values of function $G_c[(q' + 2q)\Delta\varepsilon]$, which rather wide maximum is in a point $(q' + 2q)\Delta\varepsilon = 2\pi h_2$. Thus, we obtain approximate equality:

$$2\pi r_g \frac{l}{d} + 2\pi r_g \frac{h_1}{\lambda} \approx 2\pi \frac{h_2}{\Delta\varepsilon} \quad \Rightarrow \quad h_1 \approx \lambda\left(\frac{h_2}{a} - \frac{l}{d}\right). \tag{19}$$

As $\lambda \approx Ta$, then in the last equality

$$h_1 \approx Ta\left(\frac{h_2}{a} - \frac{l}{d}\right) \approx Th_2 - \frac{Ta}{d} l$$

the integer value of h_1 is provided only at $l = 0$. With taking into account (7) it means, that of greatest intensity is the layer line (the basic layer line), located close to

$$z^* \approx \frac{h_2}{a} \approx \frac{Th_2}{\lambda} \tag{20}$$

at $h_2 > 0$, as is observed in a fig. 1.

As maxima of function $G_c[(q' + 2q)\Delta\varepsilon]$ have some width, the layer lines, getting in the appropriate interval, also have appreciable intensity (additional layer lines). Let's take differential from both parts of (19) at a constant index h_2, that is close to (20):

$$\Delta h_1 \sim -\Delta l\,, \qquad (21)$$

where the approximate equality is replaced with a mark of proportionality, as the interval of intensive layer lines depends on experimental conditions too. From (21) it is visible, that the quantity of additional layer lines is proportional to value of index l, that also is observed in a fig. 1. Addendum S_{cl}^{-} gives the similar result for $h_2 < 0$.

Addendum S_s in points (18) looks like $S_s^l = S_{sl}^{+} - S_{sl}^{-}$, where

$$S_{sl}^{+} = \sum_{q=1}^{\infty} J_{2q+1}\left(2\pi r_g \frac{h_1}{\lambda}\right) \sum_{q'=-\infty}^{\infty} i^{q'} J_{q'}\left(2\pi r_g \frac{l}{d}\right) \exp\left[-i(q'+2q+1)\varepsilon\right] G_s\left[(q'+2q+1)\Delta\varepsilon\right],$$

$$S_{sl}^{-} = \sum_{q=1}^{\infty} J_{2q+1}\left(2\pi r_g \frac{h_1}{\lambda}\right) \sum_{q'=-\infty}^{\infty} i^{q'} J_{q'}\left(2\pi r_g \frac{l}{d}\right) \exp\left[-i(q'-2q-1)\varepsilon\right] G_s\left[(q'-2q-1)\Delta\varepsilon\right].$$

Maxima of Bessel functions in S_{sl}^{+} take place under conditions: $q' \approx 2\pi r_g l/d$ and $2q + 1 \approx 2\pi r_g h_1/\lambda$, and maximum of function $G_s[(q' + 2q)\Delta\varepsilon]$ is in a point $(q' + 2q + 1)\Delta\varepsilon = 2\pi h_2$, that again gives (19) and all its consequences.

3.2. The thin radial CSR ($M < T$).

The basis for consideration of such model is the diffraction pattern in a fig. 2, which radially lengthened basal reflexes allow to speak about the small CSR sizes in this direction. In this case maxima of functions $G_0(q'\Delta\varepsilon)$, $G_c[(q' \pm 2q)\Delta\varepsilon]$ and $G_s[(q' \pm 2q \pm 1)\Delta\varepsilon]$ in (13), (14) and (15), accordingly, are narrower and intensive, than $G(2\pi Rd)$, and it is possible to be limited to their peak values.

Let's consider an addendum S_0 at peak value of q' from (17).

$$S_0(h_2) \approx i^{q'} T J_0\left(2\pi r_g \frac{h_1}{\lambda}\right) J_{q'}\left(2\pi r_g R\right) \exp\left(-iq'\varepsilon\right).$$

Main maximum of the second Bessel function takes place at

$$2\pi r_g R \approx q' = h_2 \frac{2\pi}{\Delta\varepsilon} \qquad \Rightarrow \qquad R_{h_2} \approx \frac{h_2}{a}.$$

But on the other hand summation over layers (over m) gives condition (18) again, though with a little wider maxima. However it is obvious, that in this case these two conditions are incompatible too. Hence, addendum S_0 has not essential influence on positions of strong reflexes.

A condition of a maximum of functions $G_c[(q' \pm 2q)\Delta\varepsilon]$, included in S_c, looks like:

$$\left(q' \pm 2q\right)\Delta\varepsilon = 2\pi h_2 \qquad \Rightarrow \qquad 2q = \pm\left(\frac{2\pi h_2}{\Delta\varepsilon} - q'\right),$$

and function S_c, at this condition, $S_{ch_2} = S_{ch_2}^{+} + S_{ch_2}^{-}$, where

$$S_{ch_2}^{+} = T(-1)^{Th_2} \sum_{q'=-\infty}^{\infty} i^{q'} J_{q'}\left(2\pi r_g R\right) J_{\frac{2\pi h_2}{\Delta\varepsilon} - q'}\left(2\pi r_g \frac{h_1}{\lambda}\right),$$

$$S_{ch_2}^{-} = T(-1)^{Th_2} \sum_{q'=-\infty}^{\infty} i^{q'} J_{q'}\left(2\pi r_g R\right) J_{-\frac{2\pi h_2}{\Delta\varepsilon} + q'}\left(2\pi r_g \frac{h_1}{\lambda}\right)$$

and is used: $\varepsilon/\Delta\varepsilon \approx T/2$. As before, let's write down for $S_{ch_2}^{+}$ the approximate equality from conditions of Bessel functions maxima at the peak value (18) of functions $G(2\pi Rd)$:

$$2\pi r_g \frac{h_1}{\lambda} \approx 2\pi \frac{h_2}{\Delta\varepsilon} - 2\pi r_g \frac{l}{d} \quad \Rightarrow \qquad h_1 \approx \lambda\left(\frac{h_2}{a} - \frac{l}{d}\right).$$

We again have obtained (19), that means, as in this case the basic layer line is close to z^*, determined by (20), too. However function $G(2\pi Rd)$ in this case - modulating, the positions of peaks on the layer line are determined by maxima of function $G_c[(q' + 2q)\Delta\varepsilon]$. Then, substituting in last equality the current value of argument R instead of its peak value l/d, we obtain:

$$R_{h_2}^{h_1} \approx \frac{h_2}{a} - \frac{h_1}{\lambda}.$$

This expression differs from its analogue (18) for a case of thick radial CSR in two aspects. First, the positions of strong reflexes on the layer line are determined not by "basal" interlayer spacing d, but "longitudinal" lattice parameter a. Secondly, the positions of all series displaces on distance h_1/λ at transition from one layer line to another, that is observed on the diffraction pattern in a fig. 2.

The estimation, similar to the previous item, of width of interval near the value (20), in which the additional layer lines take place, gives again expression (21), that also is observed on the diffraction pattern in a fig. 2.

Addendum S_2 from (11) gives similar expressions for other combination of indexe's h_1, h_2 and l signs.

4. CONCLUSIONS

The analysis of formation of strong reflexes from the offered multiwall circular orthogonal mixed-layer goffered nanotube's lattice model, consisting from alternating layers of type *A* and *B*, has shown:

1. All reflexes are located on system of layer lines $z^* = h_1/\lambda$, where h_1 - index of layer line (integer), and λ - period of goffering. However the greatest intensity have reflexes of basic layer lines, which are close to value z^*, appropriate to the coordinated longitudinal period a, that is $z^* = h_2/a$, where h_2 - integer.
2. At increase of the strong reflex's index l intensity of additional layer lines become appreciable, so, that the width of interval (lengthways z^*) of layer lines, having appreciable intensity, is proportional to this index.
3. In case of thick radial CSR the strong reflexes are located on the layer line as those from not goffered lattice. In case of thin radial CSR the series of strong reflexes are displaced lengthways a layer line depending on its index h_1.

ACKNOWLEDGEMENTS D.P. thanks Dr. R. Tenne for nanotube images and microdiffraction patterns.

REFERENCES

[1] G. Radovsky, R. Popovitz-Biro, M. Staiger, K. Gartsman, C. Thomsen, T. Lorenz, G. Seifert and R.Tenne, *Angew. Chem. Intl. Ed.* **50** (51), (2011) 12316-12320

[2] I.K. Nasyrov, D.M. Pashin, Z.Ya. Khalitov, D.N. Valeeva, *Scientific Israel - Technological Advantages*, **12**, 3 (2010) 63-73.

[3] O. Figovsky, D. Pashin, I. Nasyrov, Z. Khalitov, D. Valeeva, *Chemistry & Chemical Technology*, **6**, 1 (2011) 43-49.